

## Bioinspired supramolecular fibers for mercury ion adsorption†

Cite this: *J. Mater. Chem. A*, 2013, **1**, 7745Yeh-Sheng Wang,<sup>b</sup> Chih-Chia Cheng,<sup>\*b</sup> Jem-Kun Chen,<sup>d</sup> Fu-Hsiang Ko<sup>e</sup> and Feng-Chih Chang<sup>\*abc</sup>

A novel photo-cross-linkable nanofiber based on a uracil-functionalized polymer, poly[1-(4-vinylbenzyl uracil)] (PVBU), was prepared using the electrospinning technique. This PVBU nanofiber can be converted into a covalent network nanofiber through exposure to UV light at a wavelength of 254 nm. This PVBU nanofiber is able to distinguish and selectively remove mercury ions ( $\text{Hg}^{2+}$ ) from other metal ions in aqueous solution. The maximum  $\text{Hg}^{2+}$  adsorption capacity of the PVBU nanofiber is  $543.9 \text{ mg g}^{-1}$ , which is significantly higher than that of cyclic imide derivatives. The improved adsorption of  $\text{Hg}^{2+}$  allows a detection limit of less than 1 ppm, which has rarely been achieved for  $\text{Hg}^{2+}$  sensing. Furthermore, the PVBU fiber can be reused for 10 consecutive cycles using 1.0 M HCl treatment. This new material has significant potential for the simultaneous detection and separation of  $\text{Hg}^{2+}$  in environmental and industrial fields.

Received 15th March 2013

Accepted 29th April 2013

DOI: 10.1039/c3ta11072a

[www.rsc.org/MaterialsA](http://www.rsc.org/MaterialsA)

## Introduction

Heavy metal ion pollution is an issue of critical importance in the world due to its toxic effects on human health and the environment.<sup>1</sup> These heavy metals come from various industrial sources and pose serious hazards to the environment. Mercury is one of the most toxic heavy metals that can damage the central nervous system. Moreover, mercury can cause human disease due to its bioaccumulative property; long-term exposure to even minute amounts of this metal can result in severe neurological disorders and many other diseases such as kidney toxicity and chromosome breakage.<sup>2–5</sup> In the past few years, many sorbents have been developed for removing mercury ions ( $\text{Hg}^{2+}$ ) from aqueous media, such as active carbon,<sup>6</sup> ion-exchange resins,<sup>7</sup> mesoporous silica,<sup>8,9</sup> chitosan,<sup>10</sup> functionalized polymer membranes.<sup>11,12</sup> However, most of these approaches are either expensive, have low removal efficiency or lack selectivity for  $\text{Hg}^{2+}$ . Hence, there is a strong incentive to develop novel sorbents with high efficiency, selectivity and excellent regeneration capacity for  $\text{Hg}^{2+}$  removal from aqueous media.

In order to increase the adsorption capacity of sorbent materials for  $\text{Hg}^{2+}$ , many researchers have focused on two methods: (1) surface modification with functional groups and (2) increasing the surface areas of sorbent materials.<sup>13–16</sup> Recently, polymer nanofibers modified by the functional groups have attracted great attention. Polymer nanofibers prepared from the electrospinning process possess high specific surface areas and high porosities. Several examples of  $\text{Hg}^{2+}$  removal from aqueous solutions based on fibers have been reported for zonal thiol-functionalized silica nanofibers,<sup>17</sup> poly(methacrylic acid) modified cellulose acetate fibers,<sup>18</sup> wool-grafted-poly-(cyano-acetic acid  $\alpha$ -amino-acrylic-hydrazide) chelating fibers,<sup>19</sup> and 4-vinyl pyridine and 2-hydroxyethylmethacrylate grafted poly(ethylene terephthalate) fibers.<sup>20</sup> In general, these fibers do not meet the required affinity and selectivity for highly efficient removal of  $\text{Hg}^{2+}$ . Recently, Shangguan *et al.* reported that a selective binding of N-unsubstituted cyclic imides with  $\text{Hg}^{2+}$  is able to form imide–Hg–imide complexes through an imido proton–metal exchange process.<sup>21</sup> This discovery reveals the specific interaction of  $\text{Hg}^{2+}$  with the nucleobase thymine and uracil and opens a new application for sensing and removing  $\text{Hg}^{2+}$  based on cyclic imides.<sup>22–26</sup> Therefore, the ability to prepare polymer nanofibers for removing  $\text{Hg}^{2+}$  based on the specific interaction is of critical importance.

Our previous studies reported that the uracil-functionalized poly[1-(4-vinylbenzyl uracil)] (PVBU) nanofibers can be transformed into covalent network nanofibers through exposure to UV light at a wavelength of 254 nm, thereby providing an alternative route to design new and stable uracil-nanofibers from PVBU polymers.<sup>27</sup> This study has demonstrated that the PVBU nanofiber can be used in  $\text{Hg}^{2+}$  removal. This is the first example of the supramolecular nanofibers being converted into

<sup>a</sup>Department of Materials and Optoelectronic Science, National Sun Yat-Sen University, Kaohsiung 80424, Taiwan. E-mail: changfc1973@gmail.com

<sup>b</sup>Institute of Applied Chemistry, National Chiao Tung University, Hsinchu 30050, Taiwan. E-mail: chihchia.ac95g@nctu.edu.tw

<sup>c</sup>R&D Center for Membrane Technology, Chung Yuan Christian University, Chungli, Taoyuan 32043, Taiwan

<sup>d</sup>Department of Materials Science and Engineering, National Taiwan University of Science and Technology, Taipei 10607, Taiwan

<sup>e</sup>Department of Materials Science and Engineering, National Chiao-Tung University, Hsinchu 30050, Taiwan

† Electronic supplementary information (ESI) available. See DOI: 10.1039/c3ta11072a

a network formed by the selective binding of  $\text{Hg}^{2+}$  with a pair of uracil–uracil mismatch. This nanofiber exhibits significantly higher  $\text{Hg}^{2+}$  removal capacity ( $543.9 \text{ mg g}^{-1}$ ) than those presented in previous reports.<sup>29–33</sup> This PVBU nanofiber also exhibits high  $\text{Hg}^{2+}$  removal efficiency ( $10 \text{ mg g}^{-1}$ ) even in 1 ppm solution. Thus, the concentrations of  $\text{Hg}^{2+}$  can be reduced to a single digit ppm. More surprisingly, this PVBU nanofiber can be further cross-linked into shape-persistent and free-standing objects after exposure to UV light, which not only increases the dimensional stability, but also increases the reusability for removal of  $\text{Hg}^{2+}$  from aqueous environments.

## Experimental section

### Materials

Mercury dichloride was purchased from Sigma-Aldrich. *N,N*-dimethylacetamide (DMAc) was purchased from TEDIA and distilled prior to use. Poly(1-(4-vinylbenzyl)uracil) (PVBU) ( $M_n > 250\,550 \text{ g mol}^{-1}$ , PDI = 2.66) was synthesized according to our previously reported method.<sup>27</sup>

### Preparation and photo-cross-linking of PVBU nanofibers

PVBU nanofibers were fabricated by the electrospinning technique. The electrospun solution with 20 wt% concentration of PVBU in DMAc was pumped through a metal needle of 0.34 mm inner diameter at a feed rate of  $0.5 \text{ mL h}^{-1}$  using a syringe pump (KD Scientific model 100 series). A distance of 15 cm was maintained between the tip of the syringe and the collector. The high voltage of 30 kV was used to generate PVBU fibers which were collected on the surface of a grounded Al plate. The electrospun fibers of PVBU were irradiated with short-wave (254 nm) using ultraviolet cross-linkers (UVP CL-1000).

### Adsorption studies

Adsorption of  $\text{Hg}^{2+}$  from aqueous solutions on PVBU nanofibers was investigated in batch experiments. To study the effect of pH value on the adsorption of  $\text{Hg}^{2+}$ , PVBU nanofibers (5 mg) were equilibrated with  $10 \text{ mg L}^{-1}$   $\text{Hg}^{2+}$  solution at pH values of 1.5, 3.0, 5.0, 7.0, 9.0 and 11.0 and the removal efficiency  $E$  (%) was calculated according to eqn (1). The pH value of solutions was adjusted with  $\text{Na}_2\text{HPO}_3/\text{H}_3\text{PO}_4$ . For the adsorption kinetic studies, 0.05 g of PVBU nanofibers was added to 200 mL of  $20 \text{ mg L}^{-1}$   $\text{Hg}^{2+}$  solution at pH 7.0 with contact time ranging from 1 to 300 min. The effect of initial concentration of  $\text{Hg}^{2+}$  solutions was investigated in batch experiments. Different initial concentrations of  $\text{Hg}^{2+}$  aqueous solutions at pH 7.0 were equilibrated with the PVBU pristine powder, fibers and cross-linked fibers (each 5 mg) respectively. The adsorption capacity  $Q$  ( $\text{mg g}^{-1}$ ) was calculated according to eqn (2). After adsorption, the complex fibers were washed with deionized water and then dried in a vacuum. The prepared fibers were used for SEM and TEM studies.

$$E(\%) = \frac{(C_0 - C_e)}{C_0} \quad (1)$$

$$Q = \frac{(C_0 - C_e)V}{W} \quad (2)$$

where  $C_0$  and  $C_e$  are the initial and equilibrium concentration ( $\text{mg L}^{-1}$ ),  $V$  is the volume of the solution and  $W$  is the weight of the sorbent.

### Regeneration experiment

Cross-linked PVBU nanofibers (40 mg) were used for adsorbing with 40 mL of  $5 \text{ mg L}^{-1}$   $\text{Hg}^{2+}$  solution (pH 7, buffer solution) at room temperature. The equilibrium concentration was determined using an Inductive Coupled Plasma Mass Spectrometer (ICP-MS) and the removal efficiency was calculated according to eqn (1). After adsorption, the complex fibers were regenerated by using 20 mL of 1.0 M HCl solution and then washed with deionized water. The regenerated fibers were subjected to the above steps for the next cycle.

### Characterizations

The morphologies of electrospun fibers were characterized using a Field-Emission Scanning Electron Microscope (Hitachi S-4700), and the samples were sputtered with Pt before imaging. The images were taken using a microscope operating at an accelerating voltage of 15 kV. Transmission electron microscopy (TEM) images were taken using a Hitachi H-7100 electron microscope. The concentrations of  $\text{Hg}^{2+}$  and other ions in a mixed solution were measured using an ICP-MS (PE-SCIEX ELAN 6100 DRC). High-Resolution X-ray photoelectron spectroscopy data were obtained with a PHI Quantera SXM electron spectrometer from ULVAC-PHI using Al radiation. The base pressure was about  $5 \times 10^{-10}$  torr. Infrared spectra for complex fibers were measured on an attenuated reflectance Fourier transform (Nicolet 380) spectrometer.

## Results and discussion

Photo-cross-linkable PVBU uracil-functional nanofibers were prepared according to our previous study.<sup>27</sup> Fig. 1 shows the low and high magnification FE-SEM images of electrospun nanofibers from a 20 wt% concentration of PVBU/DMAc solution with an average diameter of *ca.* 250 nm. Surface area, ion-exchange and adsorption capacities are significantly increased with the decrease in the fiber diameter. Therefore, the rate of

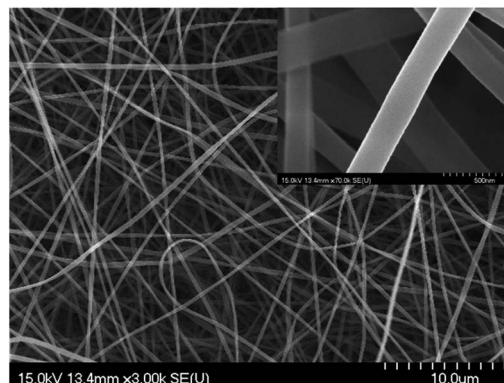


Fig. 1 FE-SEM image of electrospun PVBU nanofibers.

$\text{Hg}^{2+}$  removal is increased with the decrease of the fiber diameter. X-ray photoelectron spectrometry (XPS) and Fourier transform infrared (FT-IR) spectroscopy measurements were used to investigate the adsorption ability of  $\text{Hg}^{2+}$  and confirm the binding between uracil and  $\text{Hg}^{2+}$ .

The XPS spectra of PVBU fibers before and after  $\text{Hg}^{2+}$  adsorption are shown in Fig. 2. The survey scan of PVBU/ $\text{Hg}^{2+}$  fibers exhibits two distinguishing oxidized  $\text{Hg}4f_{7/2}$  and  $\text{Hg}4f_{5/2}$  peaks at 101.3 and 105.4 eV (Fig. 2 inset), respectively. This result indicates that mercury exists in a divalent state and subsequently binds to uracil groups as illustrated in Scheme 1. In addition, the measured atom ratios for the complexes are calculated and listed in Table 1. The atomic weight ratio of mercury and nitrogen is approximately 1 : 4, which is in good agreement with the expected theoretical ratio of the imide–Hg–imide complex.<sup>21</sup>

Fig. 3 illustrates the FT-IR spectra of PVBU and PVBU/ $\text{Hg}^{2+}$  fibers. The intensities of the N–H stretching vibrations at 2972–3300  $\text{cm}^{-1}$  are decreased upon the association of  $\text{Hg}^{2+}$ , indicating that the imido protons of PVBU are displaced by  $\text{Hg}^{2+}$ . In addition, the strong absorption band of  $\nu_{\text{C}=\text{O}}$  (imide I, 1674  $\text{cm}^{-1}$ ) shifts to a lower wavenumber of 1633  $\text{cm}^{-1}$  by ca. 40  $\text{cm}^{-1}$  which is consistent with that previously reported for platinum–imide complexes.<sup>28</sup> FT-IR spectra further reveal that the formation of the imide–Hg–imide complex results in a C=O stretching vibration shift to lower wavenumbers and the N–H stretching vibration decreases immediately.

The selectivity of PVBU fibers toward  $\text{Hg}^{2+}$  was investigated by comparing with  $\text{Co}^{2+}$ ,  $\text{Zn}^{2+}$ ,  $\text{Cu}^{2+}$ ,  $\text{Cd}^{2+}$ ,  $\text{Ca}^{2+}$ ,  $\text{Mg}^{2+}$  and  $\text{Pb}^{2+}$  respectively. As shown in Fig. 4, only  $\text{Hg}^{2+}$  shows a significant decrease in the concentration of the ICP-MS units, which is about 88% lower than its original state. This result clearly

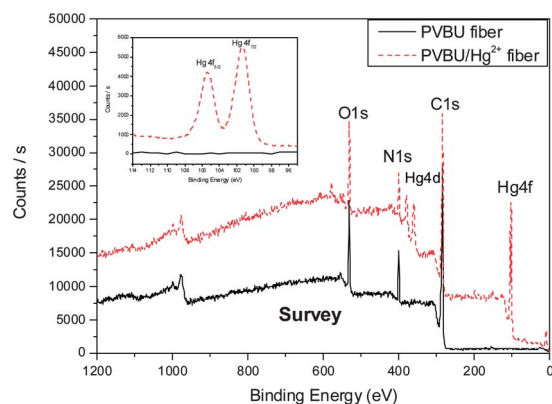
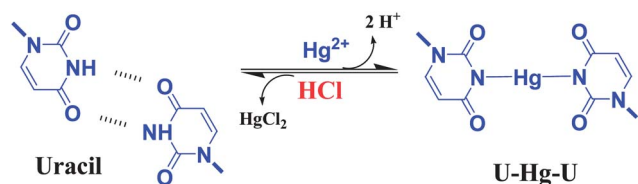


Fig. 2 XPS spectra of PVBU fibers and PVBU/ $\text{Hg}^{2+}$  fibers.



Scheme 1 Schematic representation of U–Hg–U.

Table 1 Atom ratio of the complex PVBU/ $\text{Hg}^{2+}$  fiber

	Peak (eV)	Area (CPS*eV)	Corrected RSF	Atomic (%)
Hg4f	101.3	18 069	461.6	2.5
N1s	399.8	4280	26.8	10.3
O1s	531.3	8863	39.5	14.5
C1s	284.1	18 877	16.8	72.7

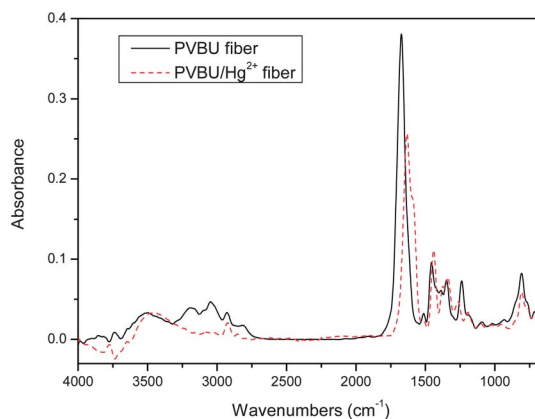


Fig. 3 FT-IR spectra of PVBU fibers and PVBU/ $\text{Hg}^{2+}$  fibers.

indicates that the PVBU fiber is able to form the specific interaction between uracil and  $\text{Hg}^{2+}$  with remarkable selectivity for  $\text{Hg}^{2+}$  over a wide variety of metal ions.<sup>34,35</sup>

The effect of pH on the adsorption of  $\text{Hg}^{2+}$  on PVBU/ $\text{Hg}^{2+}$  fibers was investigated at different pH values from 1.0 to 11.0. As shown in Fig. 5, the adsorption efficiency is extremely high at nearly 100% from pH 5.0 to 11.0, but decreases significantly as the pH is below 5.0. Shangguan *et al.* reported that a low pH value is unfavorable for dissociation of the imino protons, which reduce the coordination ability of uracil towards  $\text{Hg}^{2+}$  in aqueous solution.<sup>29</sup>

In order to understand the effect of initial concentration of the solution on the adsorption capacity of PVBU, different

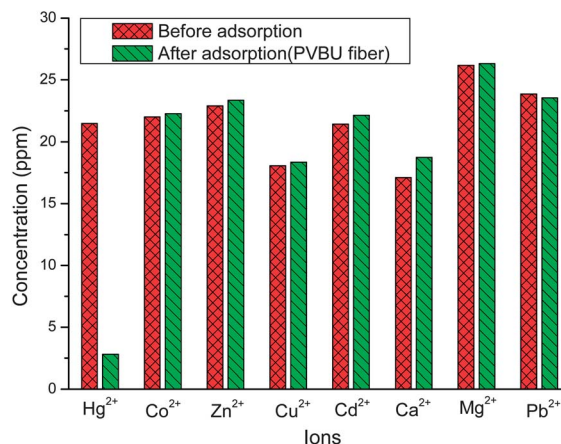
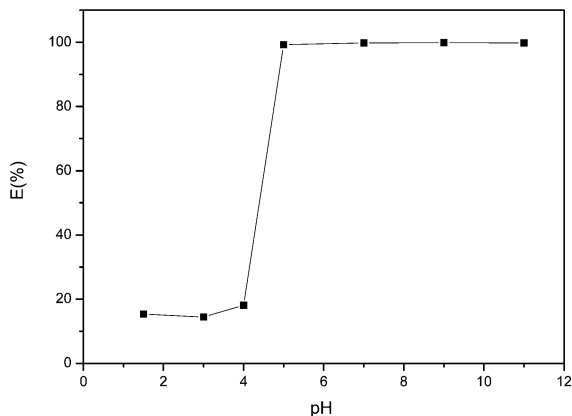
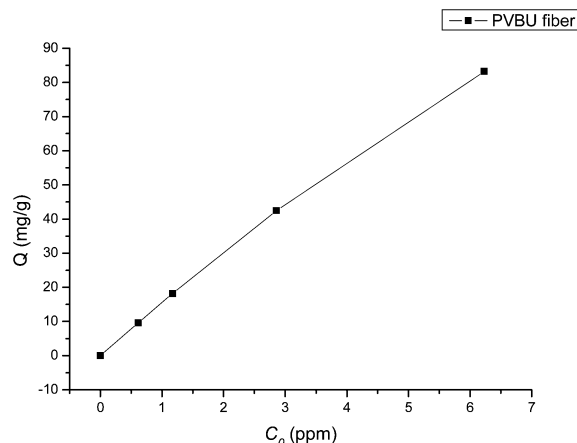


Fig. 4 Selectivity of PVBU fibers from different metal ions. Mixture solution volume: 50 mL (in pH 7.0 buffer); PVBU fibers: 10 mg.



**Fig. 5** Effect of pH on the adsorption of  $\text{Hg}^{2+}$  on PVBU fibers.  $\text{Hg}^{2+}$  concentration:  $10 \text{ mg L}^{-1}$ ; solution volume: 15 mL; PVBU fiber: 5 mg.



**Fig. 7** Adsorption curve of PVBU fibers at a low concentration of  $\text{Hg}^{2+}$ . Solution volume: 80 mL (in pH 7.0 buffer); PVBU fibers: 5 mg.

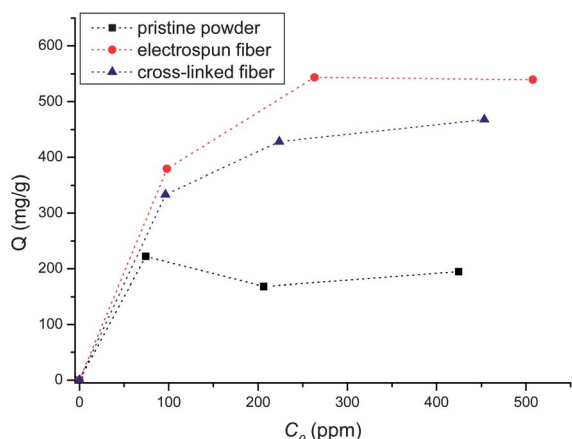


**Fig. 6** The adsorption curves of  $\text{Hg}^{2+}$  on the PVBU pristine powder, electrospun fibers and cross-linked fibers.  $C_0$  denotes the initial concentration of  $\text{Hg}^{2+}$  ppm. Solution volume: 50 mL (in pH 7.0 buffer); each sample: 5 mg.

initial concentrations of  $\text{Hg}^{2+}$  aqueous solutions were equilibrated with the PVBU pristine powder, electrospun fibers and cross-linked fibers respectively. As shown in Fig. 6, the adsorption curves of  $\text{Hg}^{2+}$  adsorbed at different initial concentrations of  $\text{Hg}^{2+}$  in aqueous solution. For PVBU fibers before and after cross-linking, the  $\text{Hg}^{2+}$  adsorption began to increase gradually with increasing  $\text{Hg}^{2+}$  concentrations. Finally the curves reached a plateau at a high concentration, which represents saturation of the active binding sites. In contrast,  $\text{Hg}^{2+}$  was less adsorbed on the PVBU pristine powder, due to the non-homogeneous morphology of the powder affecting the adsorption area. The maximum adsorption capacity of the PVBU powder, fibers and cross-linked fibers for  $\text{Hg}^{2+}$  is approximately 222.5, 543.9 and 468.1  $\text{mg g}^{-1}$  respectively. The adsorption capacities of cross-linked fibers are lower than non-cross-linked fibers, which can be attributed to the increased steric hindrance in the cross-linked fibers. However, we also found that PVBU fibers exhibited unprecedentedly higher  $\text{Hg}^{2+}$  removal capacity ( $543.9 \text{ mg g}^{-1}$ ) than the reported chitosan-coated cotton fibers ( $94.3 \text{ mg g}^{-1}$ ),<sup>30</sup> bayberry tannin-immobilized collagen fibers

( $198.49 \text{ mg g}^{-1}$ ),<sup>31</sup> thymine modified polymer sorbents ( $200 \text{ mg g}^{-1}$ ),<sup>29</sup> amine based copolymer sorbents ( $497.7 \text{ mg g}^{-1}$ )<sup>32</sup> and mercapto modified sorbents ( $522.9 \text{ mg g}^{-1}$ ).<sup>33</sup> This result is largely due to its high aspect ratio for an excellent adsorption level with high  $\text{Hg}^{2+}$  concentration, which shows that the surface density of uracil on the fiber sorbent can further increase the adsorption capacity for  $\text{Hg}^{2+}$ .

Furthermore, an excellent sorbent should display a very low detection limit and retain its selectivity for  $\text{Hg}^{2+}$ . We performed this study for low concentrations of  $\text{Hg}^{2+}$  from 0 to 7 ppm. Under this condition, high initial concentrations lead to an increase in the affinity of  $\text{Hg}^{2+}$  toward the active sites (Fig. 7). However, in the presence of  $\text{Hg}^{2+}$  concentrations even less than 1 ppm, the PVBU fiber still exhibits a high adsorption capacity of  $10 \text{ mg g}^{-1}$  for  $\text{Hg}^{2+}$ . The results showed that the PVBU fiber is able to remove most of the  $\text{Hg}^{2+}$  from water even when the concentration is down to a single digit ppm. It can be concluded that higher removal at low concentration is important in terms of likely industrial applications.

Microstructures of PVBU fibers before and after adsorption of  $\text{Hg}^{2+}$  by using the TEM images were studied (Fig. 8). We noted that, in the presence of the adsorbed  $\text{Hg}^{2+}$ , the bright white spots correspond to  $\text{Hg}^{2+}$  on the surface of PVBU/ $\text{Hg}^{2+}$  fibers (Fig. 8b). This result strongly suggests that  $\text{Hg}^{2+}$  is adsorbed onto the same active sites of the uracil group and dispersed on

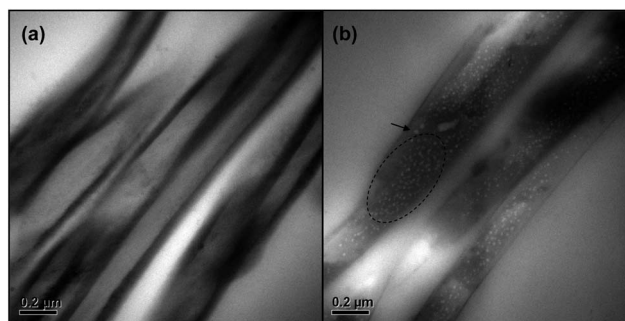


**Fig. 8** TEM images of (a) a PVBU fiber and (b) a PVBU/ $\text{Hg}^{2+}$  fiber.

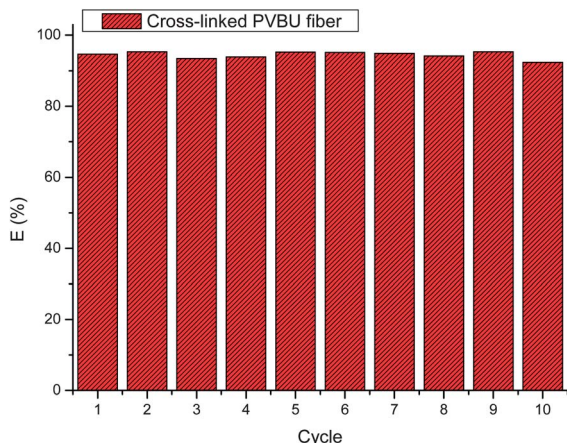


**Fig. 9** Removal efficiency of Hg<sup>2+</sup> at different regeneration cycles. Hg<sup>2+</sup> concentration 5 mg L<sup>-1</sup>; solution volume: 40 mL (in pH 7.0 buffer); cross-linked PVBU fiber: 40 mg.

the surface of PVBU fibers, which also confirmed that activated PVBU fibers have superior adsorption capacity for Hg<sup>2+</sup>.

To ensure sustainability and economic feasibility, these cross-linked PVBU/Hg<sup>2+</sup> fibers can be regenerated by 1.0 M HCl treatment without altering the adsorbent properties (Scheme 1). To test the reusability of regenerated fibers, adsorption/desorption cycles were repeated ten times with the same fiber pieces. As shown in Fig. 9, the recovery of Hg<sup>2+</sup> adsorption decreased from 94.7% in the first cycle to 92.4% in the tenth cycle. In other words, it did not decay significantly during the repeated adsorption-desorption operations, suggesting that the regenerating potency was quite effective.

## Conclusions

In summary, a novel photo-cross-linkable nanofiber for Hg<sup>2+</sup> with high adsorption, good selectivity and excellent regeneration capacities was developed by electrospinning the PVBU polymer, even though the adsorption capacity is slightly lower than non-cross-linked fibers. Improved adsorption of Hg<sup>2+</sup> allows a detection limit of less than 1 ppm to be achieved, which has rarely been achieved for Hg<sup>2+</sup> sensing elsewhere. In addition, the PVBU/Hg<sup>2+</sup> fibers can be reused for ten consecutive cycles by 1.0 M HCl treatment. We anticipate that this new material will open up substantial prospects for the selective removal of Hg<sup>2+</sup> from aqueous environments.

## Acknowledgements

This study was supported financially by the National Science Council, Taiwan (Contract no. NSC 100-2120-M-009-004).

## References

- 1 D. L. Sparks, *Elements*, 2005, **1**, 193.
- 2 J. F. Risher and C. T. De Rosa, *J. Environ. Health*, 2007, **70**, 9.
- 3 G. Guzzi and C. A. La Porta, *Toxicology*, 2008, **244**, 1.

- 4 B. Hultberg, A. Andersson and A. Isaksson, *Toxicology*, 1998, **126**, 203.
- 5 L. E. Kaercher, F. Goldschmidt, J. N. G. Paniz, É. M. M. Flores and V. L. Dressler, *Spectrochim. Acta, Part B*, 2005, **60**, 705.
- 6 G. Jyotsna, K. Kadirvelu and C. Rajagopal, *Environ. Technol.*, 2004, **25**, 141.
- 7 M. C. Dujardin, C. Vaze and I. Vroman, *React. Funct. Polym.*, 2000, **43**, 123.
- 8 L. Mercier and T. J. Pinnavaia, *Environ. Sci. Technol.*, 1998, **32**, 2749.
- 9 A. Walcarius, M. Etienne and B. Lebeau, *Chem. Mater.*, 2003, **15**, 2161.
- 10 C. P. Huang, Y. C. Chung and M. R. Liou, *J. Hazard. Mater.*, 1996, **45**, 265.
- 11 V. Smuleac, D. A. Butterfield, S. K. Sikdar, R. S. Varma and D. Bhattacharyya, *J. Membr. Sci.*, 2005, **251**, 169.
- 12 R. J. Qu, C. M. Sun, Y. Zhang, J. Chen, C. H. Wang, C. N. Ji and X. G. Liu, *J. Chem. Eng. Data*, 2010, **55**, 4343.
- 13 R. Tang, Q. Li, H. Cui, Y. Zhang and J. P. Zhai, *Polym. Adv. Technol.*, 2011, **22**, 2231.
- 14 W. Yantasee, C. L. Warner, T. Sangvanich, R. S. Addleman, T. G. Carter, R. J. Wiacek, G. E. Fryxell, C. Timchalk and M. G. Warner, *Environ. Sci. Technol.*, 2007, **41**, 5114.
- 15 J. Jimenez-Jimenez, M. Algarra, E. Rodriguez-Castellon, A. Jimenez-Lopez and J. C. G. E. da Silva, *J. Hazard. Mater.*, 2011, **190**, 694.
- 16 D. Perez-Quintanilla, I. del Hierro, M. Fajardo and I. Sierra, *J. Hazard. Mater.*, 2006, **134**, 245.
- 17 S. Z. Li, X. L. Yue, Y. M. Jing, S. S. Bai and Z. F. Dai, *Colloids Surf., A*, 2011, **380**, 229.
- 18 Y. Tian, M. Wu, R. G. Liu, Y. X. Li, D. Q. Wang, J. J. Tan, R. C. Wu and Y. Huang, *Carbohydr. Polym.*, 2011, **83**, 743.
- 19 M. Monier, N. Nawar and D. A. Abdel-Latif, *J. Hazard. Mater.*, 2010, **184**, 118.
- 20 Z. Temocin and M. Yigitoglu, *Water, Air, Soil Pollut.*, 2010, **210**, 463.
- 21 C. L. Fang, J. Zhou, X. J. Liu, Z. H. Cao and D. H. Shangguan, *Dalton Trans.*, 2011, **40**, 899.
- 22 Y. L. Tang, F. He, M. H. Yu, F. D. Feng, L. L. An, H. Sun, S. Wang, Y. L. Li and D. B. Zhu, *Macromol. Rapid Commun.*, 2006, **27**, 389.
- 23 Y. Che, X. M. Yang and L. Zang, *Chem. Commun.*, 2008, 1413.
- 24 J. Lv, C. Ouyang, X. D. Yin, H. Y. Zheng, Z. C. Zuo, J. L. Xu, H. B. Liu and Y. L. Li, *Macromol. Rapid Commun.*, 2008, **29**, 1588.
- 25 Z. Wang, D. Q. Zhang and D. B. Zhu, *Anal. Chim. Acta*, 2005, **549**, 10.
- 26 X. J. Liu, C. Qi, T. Bing, X. H. Cheng and D. H. Shangguan, *Anal. Chem.*, 2009, **81**, 3699.
- 27 Y. S. Wang, C. C. Cheng, Y. S. Ye, Y. C. Yen and F. C. Chang, *ACS Macro Lett.*, 2012, **1**, 159.
- 28 D. M. Roundhill, *Inorg. Chem.*, 1970, **9**, 254.
- 29 X. J. Liu, C. Qi, T. Bing, X. H. Cheng and D. H. Shangguan, *Talanta*, 2009, **78**, 253.
- 30 R. J. Qu, C. M. Sun, F. Ma, Y. Zhang, C. N. Ji, Q. Xu, C. H. Wang and H. Chen, *J. Hazard. Mater.*, 2009, **167**, 717.

- 31 X. Huang, X. P. Liao and B. Shi, *J. Hazard. Mater.*, 2009, **170**, 1141.
- 32 Q. F. Lu, M. R. Huang and X. G. Li, *Chem.–Eur. J.*, 2007, **13**, 6009.
- 33 S. D. Pan, H. Y. Shen, Q. H. Xu, J. Luo and M. Q. Hu, *J. Colloid Interface Sci.*, 2012, **365**, 204.
- 34 A. Ono and H. Togashi, *Angew. Chem., Int. Ed.*, 2004, **43**, 4300.
- 35 Y. Miyake, H. Togashi, M. Tashiro, H. Yamaguchi, S. Oda, M. Kudo, Y. Tanaka, Y. Kondo, R. Sawa, T. Fujimoto, T. Machinami and A. Ono, *J. Am. Chem. Soc.*, 2006, **128**, 2172.